Journal of Theoretical Biology 391 (2016) 1–12

Contents lists available at ScienceDirect

Journal of Theoretical Biology

journal homepage: www.elsevier.com/locate/yjtbi

Dynamic modeling of bone metastasis, microenvironment and therapy Integrating parathyroid hormone (PTH) effect, anti-resorptive and anti-cancer therapy

Rui Moura Coelho [a], João Miranda Lemos [b], Irina Alho [c], Duarte Valério [a], Arlindo R Ferreira [d,c], Luís Costa [d,c], Susana Vinga [a,*]

[a] IDMEC, Instituto Superior Técnico, Universidade de Lisboa, Av. Rovisco Pais 1, 1049-001 Lisboa, Portugal
[b] INESC-ID, Instituto Superior Técnico, Universidade de Lisboa, Rua Alves Redol, 9, 1000-029 Lisboa, Portugal
[c] Instituto de Medicina Molecular, Faculdade de Medicina, Universidade de Lisboa, Av. Prof. Egas Moniz, 1649-028 Lisboa, Portugal
[d] Hospital de Santa Maria, Av. Prof. Egas Moniz, 1649-035 Lisboa, Portugal

HIGHLIGHTS

- A model for bone remodeling that includes PTH is proposed.
- PTHrP is included to account for the vicious cycle of bone metastases.
- PK/PD of bisphosphonates, denosumab and chemotherapy are included as treatment.
- Model simulations illustrate how anti-cancer and anti-resorptive therapies on bone metastases can reduce tumor burden and restore bone health.

ARTICLE INFO

Article history:
Received 1 August 2015
Received in revised form
23 November 2015
Accepted 25 November 2015
Available online 4 December 2015

Keywords:
Bone remodeling
Bone metastasis
Systems biomedicine

ABSTRACT

Bone is a common site for the development of metastasis, as its microenvironment provides the necessary conditions for the growth and proliferation of cancer cells. Several mathematical models to describe the bone remodeling process and how osteoclasts and osteoblasts coupled action ensures bone homeostasis have been proposed and further extended to include the effect of cancer cells. The model proposed here includes the influence of the parathyroid hormone (PTH) as capable of triggering and regulating the bone remodeling cycle. It also considers the secretion of PTH-related protein (PTHrP) by cancer cells, which stimulates the production of receptor activator of nuclear factor kappa-B ligand (RANKL) by osteoblasts that activates osteoclasts, increasing bone resorption and the subsequent release of growth factors entrapped in the bone matrix, which induce tumor growth, giving rise to a self-perpetuating cycle known as the vicious cycle of bone metastases. The model additionally describes how the presence of metastases contributes to the decoupling between bone resorption and formation. Moreover, the effects of anti-cancer and anti-resorptive treatments, through chemotherapy and the administration of bisphosphonates or denosumab, are also included, along with their corresponding pharmacokinetics (PK) and pharmacodynamics (PD). The simulated models, available at http://sels.tecnico.ulisboa.pt/software/, are able to describe bone remodeling cycles, the growth of bone metastases and how treatment can effectively reduce tumor burden on bone and prevent loss of bone strength.

1. Introduction

Bone is a dynamic tissue that suffers constant remodeling throughout life to ensure the integrity of the skeleton. It involves tightly coordinated phenomena of bone resorption (degradation) and formation in order to preserve bone mass, undertaken by osteoclasts and osteoblasts, respectively, which form temporary structured units called *basic multicellular units* (BMUs) (Raggatt and Partridge, 2010).

* Corresponding author.
E-mail addresses: rui.coelho@tecnico.ulisboa.pt (R.M. Coelho), jlml@inesc-id.pt (J.M. Lemos), ialho@medicina.ulisboa.pt (I. Alho), duarte.valerio@tecnico.ulisboa.pt (D. Valério), ajrsferreira@gmail.com (A. Ferreira), luiscosta.oncology@gmail.com (L. Costa), susanavinga@tecnico.ulisboa.pt (S. Vinga).

http://dx.doi.org/10.1016/j.jtbi.2015.11.024
0022-5193/

Osteoclasts are multinucleated cells that result from the fusion of mononucleated hematopoietic stem and progrenitor cells that express RANK (receptor activator of NF-B) and c-fms (macrophage colony-stimulating factor receptor). In the presence of CSF-1 (colony-stimulating factor 1) and RANKL (RANK-ligand), which bind to c-fms and RANK, respectively, these cells differentiate into osteoclasts capable of bone resorption. At the end of their life cycle, osteoclasts undergo apoptosis (programmed cell death) (Raggatt and Partridge, 2010).

Bone formation results from the activity of osteoblasts, i.e. mononucleated cells able to form bone. Osteoblasts differentiation from mesenchymal stem cells (MSC) is controlled by bone morphogenetic protein (BMP), Wnt-signaling and vitamin D, among other factors. These cells express parathyroid hormone (PTH) receptors. In response to PTH, osteoblasts and cells of the osteoblastic lineage upregulate the expression of RANKL, which binds to RANK expressed in osteoclasts precursors, promoting their activation and bone resorption. These cells also produce osteoprotegerin (OPG), a soluble decoy receptor for RANKL, which inhibits osteoclastogenesis by binding to RANKL. The secretion of OPG is reduced in response to PTH, which contributes further to osteoclastogenesis. The RANK/RANKL/OPG pathway is hence of paramount importance in the regulation of bone resorption and formation. Osteoblasts can undergo apoptosis, differentiate into osteocytes or into bone lining cells (Crockett et al., 2011; Hofbauer et al., 2014).

The process of bone turnover is activated by either mechanical stimuli on the bone, or systemic changes in homeostasis which result in the production of estrogen or PTH (Raggatt and Partridge, 2010). PTH release has tonic and stochastically pulsatile components, being controlled by the calcium concentration on the parathyroid glands and eventually, by the concentration of phosphorus. It is triggered in response to a reduced calcium concentration, which increases calcium release, and inhibited when high calcium concentration is sensed (Silva and Bilezikian, 2015). The action of PTH on cells of the osteoblastic lineage results in the differentiation and activation of osteoclasts, which form a cutting cone to degrade bone, initiating the resorption phase. The resorption phase is followed by a reversal phase, where the lacunae created by bone resorption is prepared for the bone formation process, removing the undigested demineralized collagen matrix. The initiation of the formation phase is coupled to the resorption phase in a process not yet fully understood. Factors released from the bone matrix during resorption, such as insulin growth factors I and II (IGF-I,II) and TGF-β, may be involved in this coupling. However, there is evidence that, in the presence of malfunctioning osteoclasts unable to degrade bone, bone formation still takes place, leading to the hypothesis that osteoclasts produce the coupling factors, responsible for attracting osteoblasts to the sites of bone resorption (Crockett et al., 2011). Such factors include sphingosine 1-phosphate, ephrins and semaphorins (Hofbauer et al., 2014). At the resorpted site, osteoblasts commence bone formation and replace the resorpted bone by the same amount, ending the bone remodeling cycle.

Tumors have the ability to spread into organs other than its primary site, bone being a common site for metastasis. According to the “seed” and “soil” hypothesis of Paget, cancer cells (“seed”) interact with the cells of the secondary site (“soil”) in order to thrive. Primary cancer cells disseminate into circulation, often extravasating to bone, where tumor cells interact with cells in the bone marrow to grow and proliferate in the bone, by dysregulating the normal bone resorption and formation processes. These sites of cancer metastasis are usually those where bone remodeling rates are high, such as, for instance, the pelvis or the axial skeleton (Boyce, 2012; Schneider et al., 2005), or bones with abundant bone marrow (Moulopoulos and Koutoulidis, 2014).

Bone metastases are characterized as osteolytic, in case bone resorption is predominant, or osteoblastic, when bone formation is stimulated in an unstructured way, both leading to loss of bone resistance. In any case, both bone resorption and formation are present, although out of balance. Some kinds of cancer, such as breast or prostate cancer, are prone to develop bone metastases. Most metastases from breast cancer are osteolytic, whereas prostate cancer metastases are usually osteoblastic (Suva et al., 2011).

Metastatic cells stimulate bone resorption by both RANKL-dependent and RANKL-independent mechanisms. During bone resorption, TGF-β is released from the bone matrix, stimulating the production of PTH-related protein (PTHrP) by metastatic cells. PTHrP binds to the PTH receptors on cells of the osteoblastic lineage, enhancing the secretion of RANKL and subsequent activation of osteoclasts, leading to increased bone resorption. In turn, the activity of osteoclasts in the bone will result in the release of TGF-β, giving rise to a vicious cycle (Casimiro et al., 2009). TGF-β also induces the expression of interleukin-8 (IL-8) in metastatic cells, stimulating bone resorption directly by increased osteoclasts formation and activity. IL-8 can also induce IL-11, which increases osteoclasts formation via RANKL (Casimiro et al., 2009). Breast cancer metastases promote the decoupling between bone resorption and formation and the hypo-activity of osteoblasts. Bone metastases of breast cancer express dickkopf-1 (DKK-1), which inhibits the maturation and activation of osteoblasts through the Wnt signaling pathway (Voorzanger-Rousselot et al., 2007). In addition to PTHrP produced locally by metastatic cells, there is a systemic production of PTHrP at the primary tumor site, which also takes effect at the site of the metastases (Mundy and Edward, 2008).

The treatment of bone metastasis includes systemic treatment and anti-resorptive therapy for primary cancer. *Bisphosphonates* and *Denosumab* are commonly used in anti-resorptive therapy, acting in different mechanisms of bone resorption. *Bisphosphonates* are incorporated in the bone matrix, being released by bone resorption. As they are released, bisphosphonates promote the apoptosis of osteoclasts and inhibit their activity by reducing the ability to form ruffled border, essential for bone resorption (Casimiro et al., 2009). *Denosumab* is a fully human monoclonal antibody which binds exclusively to RANKL (Casimiro et al., 2009), thus increase the OPG/RANKL ratio. Anticancer treatment, such as chemotherapy and hormone therapy, targets primary cancer cells and bone metastases (Makatsoris and Kalofonos, 2009).

The processes previously described are summarized in Fig. 1.

The motivation for this work lies on creating a model with three novel features: (1) bone remodeling events are initiated by biochemical systemic regulators, namely PTH; (2) bone metastases induce a vicious cycle between metastatic growth and bone resorption, through RANKL-dependent and independent mechanisms, which includes the action of PTHrP, capable of dysregulating the bone remodeling system; and (3) relevant anticancer (chemotherapy) and anti-resorptive (bisphosphonates or denosumab) therapies for the treatment of bone metastases are included, along with the pharmacokinetics (PK) and pharmacodynamics (PD) of the drugs. Such a model would contribute to the prognosis of bone metastases and to the development of personalized therapy regimes which would better suit the needs of each patient.

The remainder of the paper is organized as follows. In Section 2, a brief review of related computational and biochemical models of bone and bone metastases is given. Section 3 presents the proposed model for bone remodeling, growth of bone metastases and treatment. In Section 4, the model is studied through simulation for different conditions, and the results are discussed according to the physiology of the disease. Finally, in

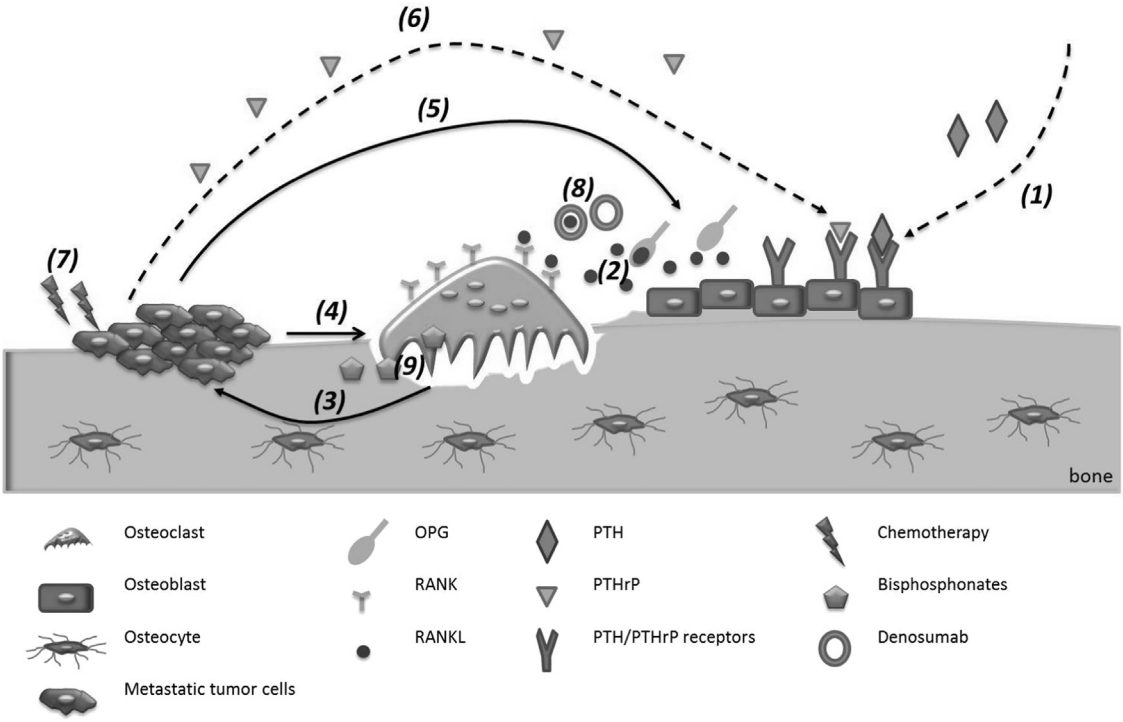

Fig. 1. Biochemical processes of bone remodeling, progression of bone metastases and treatment. *Bone remodeling:* (1) PTH stimulates RANKL production by osteoblasts; (2) RANK/RANKL/OPG pathway plays an important role in bone resorption and formation; *Bone metastases vicious cycle:* (3) Bone-derived tumor growth factors (IGFs,TGF-β, BMP, among others); (4) Tumor-derived factors stimulate bone resorption (PTHrP, TGF-β, IL-8,11, among others); (5) Tumor derived factors affect bone formation (DKK1, BMP, IGFs, among others); (6) PTHrP stimulates RANKL production by osteoblasts *Treatment:* (7) Chemotherapy directly targets cancer cells; (8) Denosumab binds to RANKL, inhibiting osteoclast formation; (9) Bisphosphonates promote osteoclast apoptosis;

Section 5, the conclusions of this work are presented, as well as possible future work.

2. Bone computational and biochemical models

Several mathematical and computational models of bone remodeling dynamics have already been proposed. In particular, models based on ordinary differential equations have been applied to analyse and simulate the biochemical interaction between the bone and tumor cells and the microenvironment.

Komarova et al. (2003) present a model for bone remodeling, described by the coupling between osteoclasts and osteoblasts using a S-system (Savageau, 1988), in which biochemical autocrine and paracrine factors are implicitly represented in the exponents. The bone mass temporal evolution is the result of the action of bone degrading osteoclasts and bone forming osteoblasts. The model is capable of representing a single remodeling cycle or a periodic behavior, with amplitude and frequency depending on the initial conditions. This is achieved by setting the autocrine and paracrine parameters to the appropriate values, triggered by a deviation in the initial conditions from the steady-state. However, since there is no evidence that bone remodeling occurs periodically at a given site, this kind of behavior is of limited use.

In Ayati et al. (2010), the same model (Komarova et al., 2003) is extended to incorporate the effect of multiple myeloma in the bone dynamics. The tumor growth is assumed to follow a Gompertz law and it affects the autocrine and paracrine parameters, dysregulating the periodic remodeling cycle and leading to a decrease in bone mass. However, this model fails to address the dependence of myeloma growth on the bone remodeling system, modeling it independently of the bone marrow microenvironment. Although treatment is suggested as step functions affecting the tumor growth and the osteoblasts apoptosis, capable of killing the tumor and restore bone mass, it does not include pharmacokinetics/pharmacodynamics.

In Komarova (2005), the single remodeling cycle behavior analyzed on the previous model of Komarova et al. (2003) is employed to study the anabolic and catabolic effects of external administration of PTH on bone remodeling. Zumsande et al. (2011) perform a bifurcation analysis on generalized bone remodeling models, applies it to the model of Komarova et al. (2003) and extends it incorporating osteoblats precursors as a variable in the system. Ryser et al. (2009) take the model in Komarova et al. (2003) and explicitly includes OPG and RANKL concentrations and their influence on the system, including the spatial evolution of a single BMU. A parameter estimation and sensitivity analysis of this model is presented in Ryser et al. (2010). The model is further extended in Ryser et al. (2012) to include the effect of bone metastases in bone remodeling and to study the ambiguous role of OPG in the system. The tumor size is included as a variable, along with the PTHrP, which binds to osteoblast thus increasing RANKL production. The tumor is also considered to directly influence the RANKL and OPG concentrations. The tumor growth is dependent on the activity of osteoclasts in the sense that it fills the cavity resulting from bone resorption. However, it considers purely osteolytic metastases, in which bone formation is completely ablated, which is not the case for most metastases, where bone formation and resorption, though dysregulated, are still present.

Lemaire et al. (2004) propose a different model for bone remodeling, explicitly incorporating the RANK/RANKL/OPG pathway, TGF-β and PTH. The interaction between bone cells, in this case osteoblast precursors, active osteoblasts and active osteoclasts, is represented through the reaction kinetics of these molecules, which can either activate or repress a mechanism for activation or differentiation. Pivonka et al. (2008) extend the previous model to include bone mass dynamics and the production of both OPG and RANKL by the two types of osteoblastic

lineage cells, and in Pivonka et al. (2010) a theoretical study on the role of the RANK/RANKL/OPG pathway in the system is performed, proposing treatment strategies for disturbances in this pathway. Wang et al. (2011) incorporate the effect of multiple myeloma on the bone remodeling system in Pivonka et al. (2008), considering the vicious cycle resulting from the interaction between the bone microenvironment and multiple myeloma cells.

Buenzli et al. (2011) add spatial evolution to the model of Pivonka et al. (2008) and Scheiner et al. (2014) include biomechanical regulation of bone remodeling and the treatment of osteoporosis by means of denosumab pharmacokinetics and effect. On a different approach, Araujo et al. (2014) use a Hybrid Cellular Automata to describe spatial and temporal interactions of bone cells and microenvironment, the vicious cycle imposed by prostate cancer metastases, and the effect of antiresorptive treatment on the bone dynamics, through bisphosphonates and anti-RANKL therapy. However, this model does not take into account systemic regulation of bone remodeling through PTH nor does it include anticancer therapy.

3. Proposed model

The model proposed here extends the one introduced by Komarova et al. (2003) by including new variables that represent the pooled concentration of PTH and PTHrP, metastatic cells and drugs used for treatment. The complete model is described as

$$\frac{dC(t)}{dt} = \alpha_1 C(t)^{g_{11}+r_{11}\frac{T(t)}{L_T}} B(t)^{g_{21}+K_{PTH_{pool_{21}}} PTH_{pool}(t)-K_{d_1}d_1(t)} - (\beta_1 + K_{d_2}d_2(t))C(t), \tag{1a}$$

$$\frac{dB(t)}{dt} = \alpha_2 C(t)^{g_{12}} B(t)^{g_{22}+r_{22}\frac{T(t)}{L_T}} - \beta_2 B(t), \tag{1b}$$

$$\frac{dPTH_{pool}(t)}{dt} = -\beta_{PTH} PTH_{pool}(t) + K_{PTH}\delta(t) + r_{PTHrP}\max\{0, C(t)-C_{th}\}\frac{T(t)}{L_T}, \tag{1c}$$

$$P(\delta(t)=1) = 1 - \exp\left(-\left(\frac{t}{\lambda_W}\right)^{k_W}\right), \tag{1d}$$

$$\frac{dT(t)}{dt} = k_T \max\{0, C(t)-C_{th}(t)\}\frac{T(t)}{\lambda_T + T(t)} - K_{d_3}d_3(t)T(t), \tag{1e}$$

$$\frac{dz(t)}{dt} = -k_1 \max\{0, C(t)-C_{th}\} + k_2 \max\{0, B(t)-B_{th}\}, \tag{1f}$$

$$\frac{dC_{th}(t)}{dt} = \alpha_1 C_{th}(t)^{g_{11}+r_{11}\frac{T(t)}{L_T}} B_{th}(t)^{g_{21}-K_{d_1}d_1(t)} - (\beta_1 + K_{d_2}d_2(t))C_{th}(t), \tag{1g}$$

$$\frac{dB_{th}(t)}{dt} = \alpha_2 C_{th}(t)^{g_{12}} B_{th}(t)^{g_{22}+r_{22}\frac{T(t)}{L_T}} - \beta_2 B_{th}(t). \tag{1h}$$

The description for the variables and parameters included in the model is given in Table 1.

The bone mass z is affected by the number of bone degrading osteoclasts, C, and bone forming osteoblasts, B. According to the model, bone resorption and formation rates are proportional to the number of active osteoclasts and osteoblasts, which is given by $\max\{0, C-C_{th}\}$ and $\max\{0, B-B_{th}\}$, respectively. The number of osteoclasts and osteoblasts which are above the thresholds set by variables C_{th} and B_{th}, respectively, are considered to be active. Constants k_1 and k_2 represent bone resorption and formation activity and are chosen such that, in normal conditions, the bone mass returns to its initial value after a bone remodeling cycle.

Both osteoclasts and osteoblasts produce regulatory factors that affect their own or the other cell type production, denominated autocrine (g_{11}, g_{22}) and paracrine factors (g_{12}, g_{21}), respectively. In particular, the RANK/RANKL/OPG pathway is encoded in g_{21}, as the ratio of RANKL and OPG produced by osteoblasts has a paracrine effect on the regulation of osteoclasts. The production and death rate of the cells are, respectively, encompassed by α_i and β_i, $i=1$ for osteoclasts and $i=2$ for osteoblasts.

Considering only C, B and z, by setting the state variables PTH_{pool} and T and variables d_1, d_2 and d_3 to 0, the system (1) reduces to that in Komarova et al. (2003), on which an analysis on the possible values and resulting dynamics for the parameters has already been performed. In this model, the set of parameters is selected such that the system exhibits a stable steady-state

Table 1
Description of variables and parameters used in model (1).

Variable	Description	Units
C	Number of osteoclasts	cells
B	Number of osteoblasts	cells
PTH_{pool}	PTH/PTHrP concentration variation	ng/L
T	Bone metastases size	%
z	Bone mass	%
d_1	Effect of denosumab	–
d_2	Effect of bisphosphonates	–
d_3	Effect of anti-cancer therapy	–
C_{th}	Threshold for active osteoclasts	cells
B_{th}	Threshold for active osteoblasts	cells
Parameter	Description	Units
α_1	Osteoclasts activation rate	$\text{cell}^{-1}\,\text{day}^{-1}$
α_2	Osteoblasts activation rate	$\text{cell}^{-1}\,\text{day}^{-1}$
β_1	Osteoclasts apoptosis rate	day^{-1}
β_2	Osteoblasts apoptosis rate	day^{-1}
g_{11}	Osteoclasts autocrine regulator	–
g_{21}	Osteoblasts-derived osteoclasts paracrine regulator	–
g_{12}	Osteoclasts-derived osteoblasts paracrine regulator	–
g_{22}	Osteoblasts autocrine regulator	–
k_1	Bone resorption rate	$\%\,\text{cell}^{-1}\,\text{day}^{-1}$
k_2	Bone formation rate	$\%\,\text{cell}^{-1}\,\text{day}^{-1}$
K_{PTH}	PTH growth rate	$\text{ng L}^{-1}\,\text{day}^{-1}$
β_{PTH}	PTH/PTHrP degradation rate	day^{-1}
$K_{PTH_{pool_{21}}}$	Influence of PTH/PTHrP in RANKL/OPG ratio	$\text{ng}^{-1}\,\text{L}$
k_W	Shape parameter of Weibull distribution	–
λ_W	Scale parameter of Weibull distribution	–
k_T	Bone metastases growth rate through bone resorption	$\%\,\text{cell}^{-1}\,\text{day}^{-1}$
λ_T	Half-saturation constant for bone metastases size	%
L_T	Maximum size of bone metastases	%
r_{11}	Effect of tumor in osteoclasts autocrine regulator	–
r_{22}	Effect of tumor in osteoblasts autocrine regulator	–
r_{PTHrP}	Rate of PTHrP production by cancer cells	$\text{ng L}^{-1}\,\text{cell}^{-1}\,\text{day}^{-1}$
C_0	Initial number of osteoclasts	cells
B_0	Initial number of osteoblasts	cells
z_0	Initial bone mass percentage	%
PTH_{pool_0}	Initial PTH/PTHrP concentration	ng/L
T_0	Initial size of bone metastases	%
K_{d_1}	Maximum effect of denosumab	–
K_{d_2}	Maximum effect of bisphosphonates	day^{-1}
K_{d_3}	Maximum effect of anti-cancer therapy	$\%\,\text{day}^{-1}$
D_0	Drug dosage	mg
τ	Administration time interval	day
k_e	Drug elimination rate	day^{-1}
k_a	Drug absorption rate	day^{-1}
F	Bioavailability	–
V_d	Volume distribution	L
C_{50}	Drug concentration for 50% of maximum effect	mg/L

$(C_{ss}, B_{ss}, P_{ss} = 0)$, and, when in steady-state, the RANKL/OPG ratio inhibits the activation of osteoclasts, that is, $g_{21} < 0$. All other autocrine and paracrine parameters are positive, with g_{11} and g_{22} chosen such that the system is stable. In healthy bone, $C_{ss} = \left(\frac{\beta_1}{\alpha_1}\right)^{(1-g_{22})/\Gamma}\left(\frac{\beta_2}{\alpha_2}\right)^{g_{21}/\Gamma}$ and $B_{ss} = \left(\frac{\beta_1}{\alpha_1}\right)^{g_{12}/\Gamma}\left(\frac{\beta_2}{\alpha_2}\right)^{(1-g_{11})/\Gamma}$, where $\Gamma = g_{12}g_{21} - (1-g_{11})(1-g_{22})$ (see Komarova et al., 2003).

PTH acts as a systemic regulator of bone remodeling, whose variation of concentration is incorporated in PTH_{pool}, which represents the joint concentration of PTH and PTHrP. PTH binds to PTH receptors expressed in osteoblasts, resulting in an upregulation of RANKL, which leads to the formation and activation of osteoclasts, thus initiating the remodeling cycle. The paracrine parameter g_{21} represents the RANKL/OPG ratio and so it is affected by PTH by adding the term $K_{PTH_{pool_{21}}} PTH_{pool}$ to the exponent, where $K_{PTH_{pool_{21}}} > 0$ represents the increase in RANKL caused by the presence of PTH/PTHrP.

Unlike Komarova et al. (2003), the remodeling cycle is not initiated by a change in initial conditions. Instead, there is a *triggering signal* δ, a pulse of amplitude and width 1, resulting from a systemic change in the bone microenvironment, which results in the production of PTH, which is then responsible for the recruitment of osteoclasts, as previously explained. Since different BMUs can be activated simultaneous and asynchronously, the production of PTH is triggered at time instants that follow a Weibull distribution. The cumulative distribution function for the Weibull distribution is $W(t; k_W, \lambda_W) = 1 - \exp(-(\frac{t}{\lambda_W})^{k_W})$, where $t \geq 0$ represents time, $k_W > 0$ is the shape parameter and $\lambda_W > 0$ the scale parameter. The probability of triggering a remodeling event $P(\delta(t) = 1)$ depends on the time elapsed since the last one occurred, according to parameters λ_W and k_W, increasing over time. Constant β_{PTH} represents the natural decay of the concentration of PTH/PTHrP, which, together with constant K_{PTH}, controls the peak value of PTH_{pool} in healthy bone remodeling.

In presence of metastatic cells, the bone remodeling dynamics is dysregulated. T represents the relative size of the metastases (in percentage), with maximum allowed size $L_T = 100\%$. As in Ayati et al. (2010), metastatic cells influence directly the autocrine parameters in osteoclasts and osteoblasts, promoting the production of osteoclasts, encoded by the term $r_{11}\frac{T}{L_T}$, and inhibiting the activation of osteoblasts through $r_{22}\frac{T}{L_T}$, where $r_{11} > 0$ and $r_{22} < 0$ reflect the direct influence of the cancer cells in this dysregulation. Similarly to Ayati et al. (2010), the thresholds C_{th} and B_{th} are affected by the presence of the tumor. However, while in Ayati et al. (2010) this dependence was binary, in the sense that there were two threshold values, one for the absence of tumor (computed with $T(t) = 0$) and another for the presence of tumor (computed with $T(t) = L_T$), here the threshold changes, generalizing the former proposal, as to accommodate the dynamic evolution of T.

Furthermore, cancer cells produce PTHrP in the presence of TGF-β, released during bone resorption. Osteoblasts receptors for PTH and PTHrP are the same and so PTHrP stimulates the production of RANKL in osteoblasts. Hence, PTHrP can be incorporated also in PTH_{pool}, adding the term $r_{PTHrP} \max\{0, C - C_{th}\}T$ to the dynamics of PTH_{pool}, to represent the effect of TGF-β released from the bone matrix during resorption, proportional to the resorption rate $\max\{0, C - C_{th}\}$, in the secretion of PTHrP by the cancer cells, T. There is also a systemic production of PTHrP at the primary tumor site which affects locally the site of bone metastasis. However, since the primary tumor is not explicitly represented, this component was not included in the model, although the qualitative effect of adding a systemic production PTHrP to the model is nevertheless present through parameter g_{21}.

The growth of metastatic cancer cells is dependent on growth factors released during resorption (although, in latter stages, this growth may become autonomous of the bone microenvironment, which is not included in this model), so the growth rate is proportional to bone resorption, $\max\{0, C - C_{th}\}$, by the tumor growth rate constant k_T. The growth rate is also affected by a sigmoid term $\frac{T}{\lambda_T + T}$, representing the effect of the current extension of the metastasis on its own growth, λ_T being the half-saturation constant. This term reflects the fact that, while bone resorption may have little effect on the growth rate when the metastasis is much smaller than λ_T, this effect increases quickly as the size increases, being then limited only by the bone resorption. Tumor growth is also driven by other factors independent of resorption, such as oestrogen, however these are not included in the model.

The effect of denosumab, d_1, bisphosponates, d_2, and anti-cancer therapy, d_3, is included in the model, acting on the appropriate mechanisms.

Denosumab acts as a decoy receptor for RANKL, lowering the RANKL concentration and hence the activation of osteoclasts. As such, the term $-K_{d_1} d_1$ is added to exponent g_{21}, to represent the inhibition of RANKL produced by osteoblasts. Bisphosphonates lay on the bone matrix, being released and absorbed by osteoclasts as they degrade bone, leading to inhibition of bone resorption and promoting their apoptosis. In this model, bisphosphonates are only considered to promote apoptosis of osteoclasts by adding the term $K_{d_2} d_2$ to β_1. Anti-cancer therapy directly targets cancer cells and promotes their apoptosis. It is possible to use combination or single agent chemotherapy in the treatment of bone metastases. As such, the term $-K_{d_3} d_3 T$ is added to the expression of tumor growth to represent the effect of anti-cancer therapy, d_3, in the killing of the tumor. Constants K_{d_1}, K_{d_2} and K_{d_3} represent the maximum effect of denosumab, bisphosphonates and anti-cancer therapy, respectively. Similarly to the case of the presence of cancer cells, the thresholds C_{th} and B_{th} are affected by the treatment variables in the appropriate terms.

The effect of a drug, $d(t)$, with respect to its concentration in the plasma is given by it pharmacodynamics, which can be expressed by a Hill function as

$$d(t) = \frac{C_p(t)}{C_{50}(t) + C_p(t)}, \tag{2}$$

where C_p is the concentration of the drug in the plasma and C_{50} is the concentration that achieves 50% of the maximum effect. This effect is bounded between 0 and 1, where 0 corresponds to no effect and 1 to the maximum effect of the drug, which is then scaled appropriately when included in the complete model.

The pharmacokinetic (PK) model used is a one-compartment model with first-order absorption and elimination for subcutaneous administration for denosumab and intravenous (IV) administration for bisphosphonates (zoledronic acid) and chemotherapy (paclitaxel) (Dhillon and Kostrzewski, 2006). For subcutaneous administration, the concentration of drug remaining to be absorbed, C_g, and the effective drug concentration in the plasma, C_p, are described by

$$\frac{dC_g(t)}{dt} = -k_a C_g(t), \tag{3}$$

$$\frac{dC_p(t)}{dt} = k_a C_g(t) - k_e C_p(t), \tag{4}$$

where k_a and k_e are the absorption and elimination rate, respectively.

For multiple dose subcutaneous administration, assuming a fixed administration time interval τ of dose D_0, which gives the initial plasma concentration $C_p^0 = \frac{D_0 F}{V_d}$, where V_d is the volume distribution and F the bioavailability, the drug concentration after the

Table 2
Parameters for bone remodeling and bone metastases in model (1). The values for α_1, α_2, β_1, $\beta 2$, g_{11}, g_{21}, g_{12}, g_{22}, k_1 and k_2 were obtained from Komarova et al. (2003) and Ayati et al. (2010). The remainder of the parameters are introduced in this work.

Parameter	Value
α_1	3
α_2	4
β_1	0.2
β_2	0.02
g_{11}	0.1
g_{21}	-1
g_{12}	0.8
g_{22}	0.2
k_1	0.5
k_2	0.00248723
K_{PTH}	1
β_{PTH}	0.1
$K_{PTH_{pool_{21}}}$	1.261
k_W	15
λ_W	300
k_T	1
λ_T	10
L_T	100
r_{11}	0.022
r_{22}	-0.198
r_{PTHrP}	0.0043
C_0	C_{ss}
B_0	B_{ss}
z_0	100
PTH_{pool_0}	0
T_0	1

nth dose, $C_p(n,t')$, is described by

$$C_p(n,t') = C_p^0 \frac{k_a}{k_a-k_e}\left(\frac{1-e^{-nk_e\tau}}{1-e^{-k_e\tau}}e^{-k_e t'} - \frac{1-e^{-nk_a\tau}}{1-e^{-k_a\tau}}e^{-k_a t'}\right), \quad (5)$$

where $t' = t-(n-1)\tau$ represents the time elapsed after the nth dose. After a large number of doses, the system will reach the steady-state of average $\overline{C}_{p_{ss}} = \frac{1}{\tau}\frac{C_p^0}{k_e}$.

The pharmacokinetics for single IV administration is given by

$$\frac{dC_p(t)}{dt} = -k_e C_p(t), \quad (6)$$

where the initial dose D_0 is included in the initial condition of C_p as $C_p^0 = \frac{D_0}{V_d}$.

4. Results and discussion

The bone remodeling model proposed in Section 3 was simulated in MATLAB Simulink for different conditions, namely for healthy bone remodeling (Section 4.1), then in the presence of metastatic cells (Section 4.2), and finally with the inclusion of therapy (Section 4.3). The values for the parameters used, unless stated otherwise, are the ones described in Tables 2 and 3. The model developed is available at http://sels.tecnico.ulisboa.pt/software/.

4.1. Healthy bone remodeling

The dynamic response of system (1) in the absence of metastatic cells is presented in Fig. 2, with the parameters set according to Table 2, except that $T_0 = 0$, and the variables corresponding to treatment d_1, d_2 and d_3 are equal to 0.

The concentration of PTH increases at certain time instances, following a Weibull distribution, which leads to an upregulation of RANKL in osteoblasts. The number of osteoclasts increases due to this production of RANKL, initiating the remodeling cycle. As

Table 3
Parameters for therapy in model (1): denosumab, d_1, bisphosphonates, d_2 (zoledronic acid) and anti-cancer therapy, d_3 (paclitaxel). The PK parameters, D_0, τ, k_e, k_a, F and V_d, for denosumab, zoledronic acid and paclitaxel can be, respectively, found in Gibiansky et al. (2012), Chen et al. (2002) and Perez et al. (2001). The PD parameters, C_{50} and K_d, were chosen through simulation.

Parameter	d_1	d_2	d_3
D_0	120	4	176
τ	28	28	7
k_e	0.0248	0.1139	1.2797
k_a	0.2568	–	–
F	0.62	–	–
V_d	3.1508	536.3940	160.2570
C_{50}	1.2	0.0001	0.002
K_d	0.48	1.2	0.017

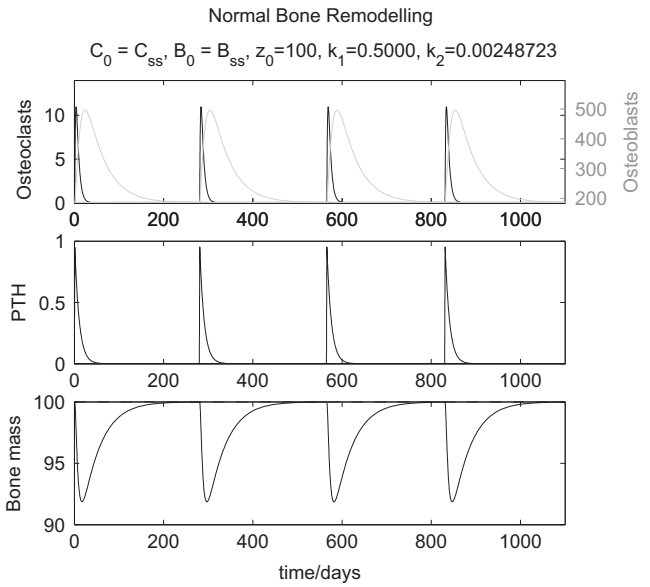

Fig. 2. Bone remodeling activated by PTH.

PTH_{pool} goes to 0, that is, PTH concentration returns to its normal value, the system starts to converge to its steady-state value (see Haden et al., 2000 for PTH normal values according to age and gender). When the steady-state is reached, it is considered that the lifetime of the BMU is over and the remodeling cycle has ended. Nonetheless, the recruitment of BMUs for bone remodeling can restart at any given time, even if other BMUs are still active. In Fig. 2, four BMUs are activated at distinct time instants, following a Weibull distribution, controlled by k_w and λ_W, and therefore not periodically. For visualization purposes, these parameters were chosen such that the lifecycles of each BMU would not overlap. While active, the BMUs start by degrading bone through the action of osteoclasts, as it can be observed in the plot for bone mass, followed by a period of bone formation carried out by active osteoblasts, restoring the bone mass to its initial value. In the absence of cancer cells and treatment, the thresholds C_{th} and B_{th} do not change over time and are equal to the steady states C_{ss} and B_{ss}, respectively.

4.2. Bone metastases

Cancer cells influence the bone remodeling cycle by directly and indirectly influencing the activity of the bone cells. First, the direct influence of the tumor in the autocrine parameters is studied, by setting $r_{PTHrP} = 0$. The trace of the Jacobian, J, of the system composed by C and B in the absence of the tumor, computed at the

steady-state (C_{ss}, B_{ss}), is $\mathrm{tr}(J)=\beta_1(g_{11}-1)+\beta_2(g_{22}-1)$ (Komarova et al., 2003), and its value determines the type of stability of the steady-state. The set of parameters r_{11} and r_{22} is chosen such that the trace, and hence the stability of the new steady-state resultant from the inclusion of the tumor, remains unchanged. The trace of the subsystem including the tumor, $\mathrm{tr}(J_T)$, is given by

$$\mathrm{tr}(J_T)=\beta_1\left(g_{11}+r_{11}\frac{T(t)}{L_T}-1\right)+\beta_2\left(g_{22}+r_{22}\frac{T(t)}{L_T}-1\right)$$
$$=\mathrm{tr}(J)+\beta_1 r_{11}\frac{T(t)}{L_T}+\beta_1 r_{22}\frac{T(t)}{L_T} \quad (7)$$

For the trace to remain unchanged,

$$\mathrm{tr}(J_T)=\mathrm{tr}(J)$$
$$\Rightarrow r_{22}=-\frac{\beta_1}{\beta_2}r_{11} \quad (8)$$

Since the tumor directly stimulates osteoclast and inhibits osteoblast formation, through, for instance, IL -1 and DKK -1, r_{11} should be positive and r_{22} negative, which is satisfied by Eq. (8). The values of r_{11} (and hence r_{22}) are chosen through simulation so that the number of active osteoclasts increases, while the number of active osteoblasts is unaltered or decreases, when in comparison to healthy bone remodeling, as to represent osteolytic metastases (Casimiro et al., 2009).

In Fig. 3a, the effect of the metastasis in the autocrine parameters is studied, by setting the tumor variable to a constant value of L_T, its maximum size, $r_{PTHrP}=0$ and running the model for different values of r_{11}, which defines r_{22}. The remaining parameters are left unchanged and according to Table 2.

For increasing values of r_{11} and, consequently, lower values of r_{22}, there is an increase in the number of recruited osteoclasts and a downregulation in the activation of osteoblasts, resulting in a reduction of bone mass which the osteoblasts cannot account for. For r_{11} values above 0.2, it can be observed in Fig. 3 that bone formation is ablated, representing cases of purely osteolytic metastases. The thresholds C_{th} and B_{th} for the bone mass change as the tumor evolves, reaching greater values for osteoclasts and lower ones for osteoblasts.

Constant r_{PTHrP} plays a key role in determining the dynamics of the system in presence of the tumor. The inclusion of the corresponding term introduces a new unstable equilibrium point, which can be found numerically. Setting the tumor size to L_T, the influence of r_{PTHrP} on the dynamics of the system is represented in Fig. 3, for $r_{11}=r_{22}=0$. Again, the remainder of the parameters are set according to Table 2.

From Fig. 3b, it becomes clear that the number of active osteoclasts and osteoblasts in a remodeling cycle increases with r_{PTHrP}. An important effect of constant r_{PTHrP} is that it can extend the duration of a remodeling cycle. As it can be observed from Fig. 3b, it is possible to choose values for this constant that would extend the lifespan of a BMU, more specifically, the time during which the bone is being degraded. This corresponds to the vicious cycle imposed by the metastatic cells, which maintain the bone resorption period in order to grow (Casimiro et al., 2009).

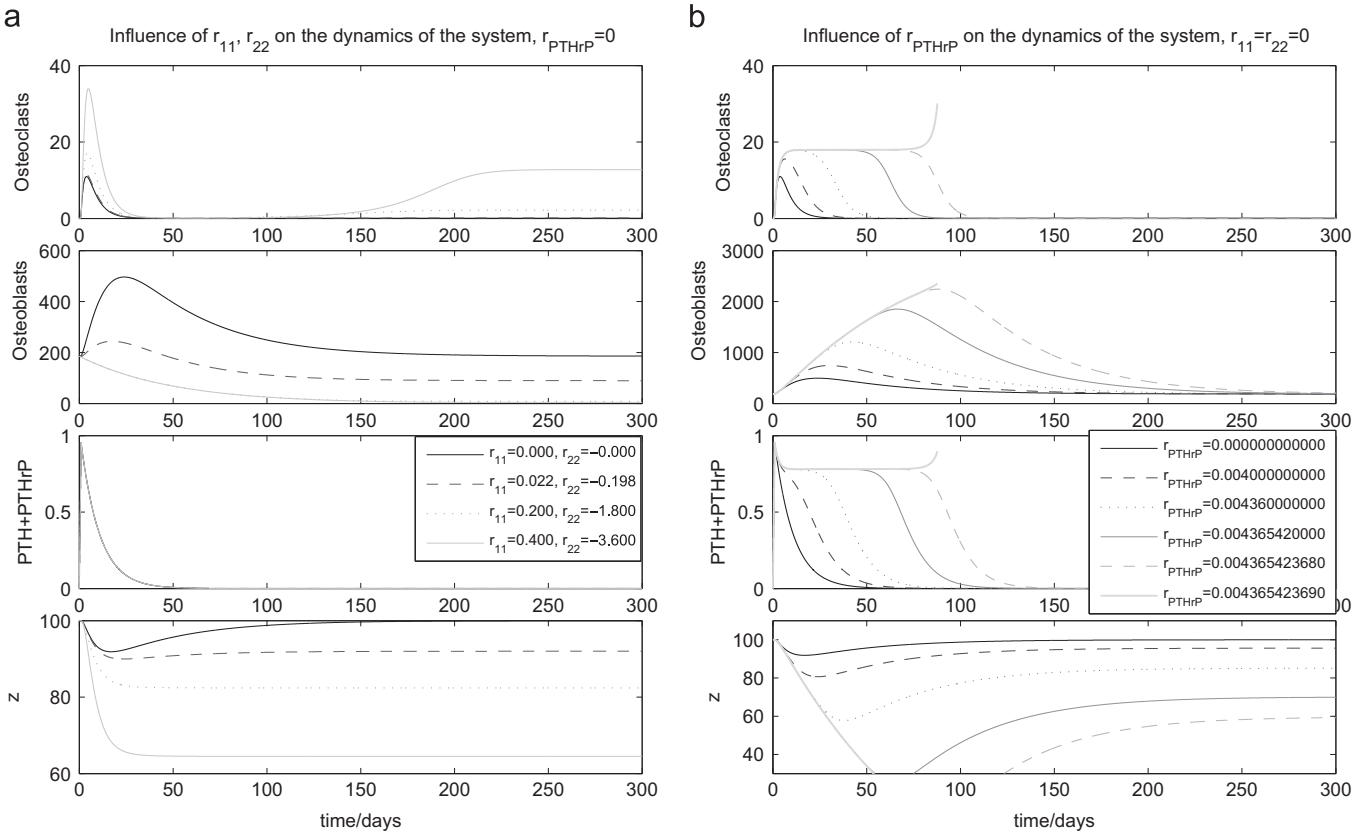

Influence of r_{11} and r_{22} on the dynamics of the system in presence of metastasis, $r_{PTHrP}=0$.

Influence of r_{PTHrP} on the dynamics of the system in presence of metastasis, $r_{11}=r_{22}=0$.

Fig. 3. Influence of bone metastases parameters on bone remodeling.

Increasing this value, one will eventually reach a situation where the system becomes unstable and no longer converges, as it can be observed in Fig. 3 for the light-gray full line. Through simulation, it is possible to determine a lower bound for the value of r_{PTHrP} above which the system becomes unstable; the full analytical study of this behavior could be further investigated in the future.

In the presented case, the final bone mass after a remodeling cycle will decrease due to the predominant action of osteoclasts over osteoblasts, despite both resorption and formation increase. However, by changing the value of g_{12}, it is possible to reach similar results in terms of lifespan extension of the BMU, but with final bone mass equal to or greater than the initial bone mass, as described in Komarova (2005). Physiologically, it is expected that an increase in PTHrP would result in higher bone resorption than bone formation for osteolytic metastases, so the value of g_{12} was chosen accordingly. For these set of parameters, g_{12} could be chosen from 0 to 0.6 to achieve such results, where 0.6 leads to a null relative change in bone mass after a remodeling cycle. Higher values result in predominant bone formation over resorption, characteristic of osteoblastic metastases.

The results from simulating the model including tumor metastasis are presented in Fig. 4, with the parameters and initial conditions of Table 2. The values for r_{11}, r_{22} and r_{PTHrP} were selected based on the previous simulations, such that there would be a general increase in bone activity, although with a predominance of bone resorption over formation.

It is possible to observe in Fig. 4 that tumor growth occurs only during bone resorption taken by osteoclasts, as part of the simplification of not accounting for other factors that drive tumor growth (e.g., oestrogen). As the tumor grows, more PTHrP is secreted by the cancer cells to stimulate the production of RANKL by osteoblasts, resulting in increased bone activity of predominant resorption, further contributing to the growth of the tumor (whose size is limited to L_T) and leading to a decrease in bone mass.

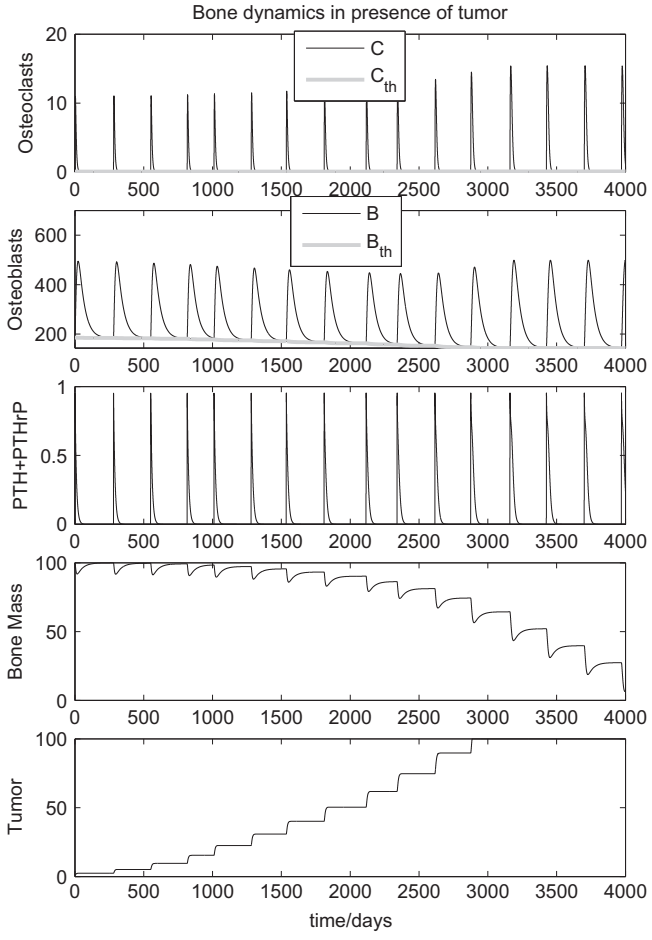

Fig. 4. Bone dynamics and metastatic growth as co-dependent mechanisms.

4.3. Treatment for bone metastases

To study the effect of anti-resorptive treatment, the full model was simulated for various values of maximum effect of denosumab, K_{d_1}, and bisphosphonates, K_{d_2}, for $d_1 = d_2 = 1$, meaning that the drug concentration administrated achieves the maximum effect, in the cases where the tumor is absent, $T=0$, and the tumor has reached its maximum size, $T = L_T$. The bone mass evolution for the different scenarios is presented in Fig. 5.

On the left and right column, respectively, the effect of denosumab and bisphosphonates on the bone mass, for $T=0$ (top) and $T = L_T$ (bottom), is represented for the different effects of the drugs applied to the system. For both drugs, the increase in drug effect reveals a decrease in bone resorption, which would result in a decrease in tumor growth. Analysing the effect of denosumab, K_{d_1} (left column in Fig. 5), it can be observed that for $T=0$ (top figure), the bone mass greatest increase is achieved for an effect of $K_{d_1} = 0.210$, not for the highest effect $K_{d_1} = 3.000$. In fact, the curve corresponding to the highest effect presents a very low increase in bone formation, resulting from the almost complete annihilation of bone resorption, to which bone formation is coupled. The same happens for bisphosphonates, as it can be observed from the top-right figure, where the greatest bone formation is achieved for an effect $K_{d_2} = 1.204$ and not for the highest effect of 53.496. There is no clinical evidence that higher drug effects would result in a decreased performance in bone formation, though, since higher doses are not tested in practice.

Nonetheless, the effect that leads to the highest increase in bone mass in the absence of cancer cells (for denosumab, $K_{d_1} = 0.210$, Fig. 5, top-left; for bisphosphonates, $K_{d_2} = 1.024$, Fig. 5, top-right) is different from the optimal value if tumor cells are present (for denosumab, $K_{d_1} = 0.480$, Fig. 5, bottom-left; for bisphosphonates, $K_{d_2} = 3.477$, Fig. 5, bottom-right), which corresponds to a greater inhibition of bone resorption.

These results raise the hypothesis that different dosages should be administrated according to the disease burden in bone, in order to achieve decreased bone resorption and maximized formation. However, in reality such a high bone gain is not achieved. As previously mentioned when studying the effect of r_{PTHrP} on the system, the outcome of bone remodeling is highly dependent on the value of g_{12} (Komarova, 2005). As such, different choices for this parameter can result in a more conservative bone gain, which was not fully studied in this work.

To achieve a higher effect, the dosage and frequency of drug intake must be higher, according to the Eq. (2) describing the pharmacodynamics. In turn, the toxicity of the treatment introduced in the system would increase, which is not desirable. As such, a control law to regulate the administered drug concentration could be developed to maximize the bone formation and minimize toxicity and tumor progression at its the different disease burden, although that is out of the scope of this work.

The PK/PD of each drug for multiple dose administration is shown in Fig. 6, according to the parameters in Table 3. Fig. 6a–c represents the PK and PD for denosumab (C_{p_1}, d_1), bisphosphonates (C_{p_2}, d_2) and paclitaxel (C_{p_3}, d_3), respectively, where the treatment starts at $t=1$ day and stops at $t=300$ days for denosumab and bisphosphonates, and at time $t=30$ days for paclitaxel, for visualization purposes. It can be observed that the steady-state concentration has been reached before the treatment is interrupted.

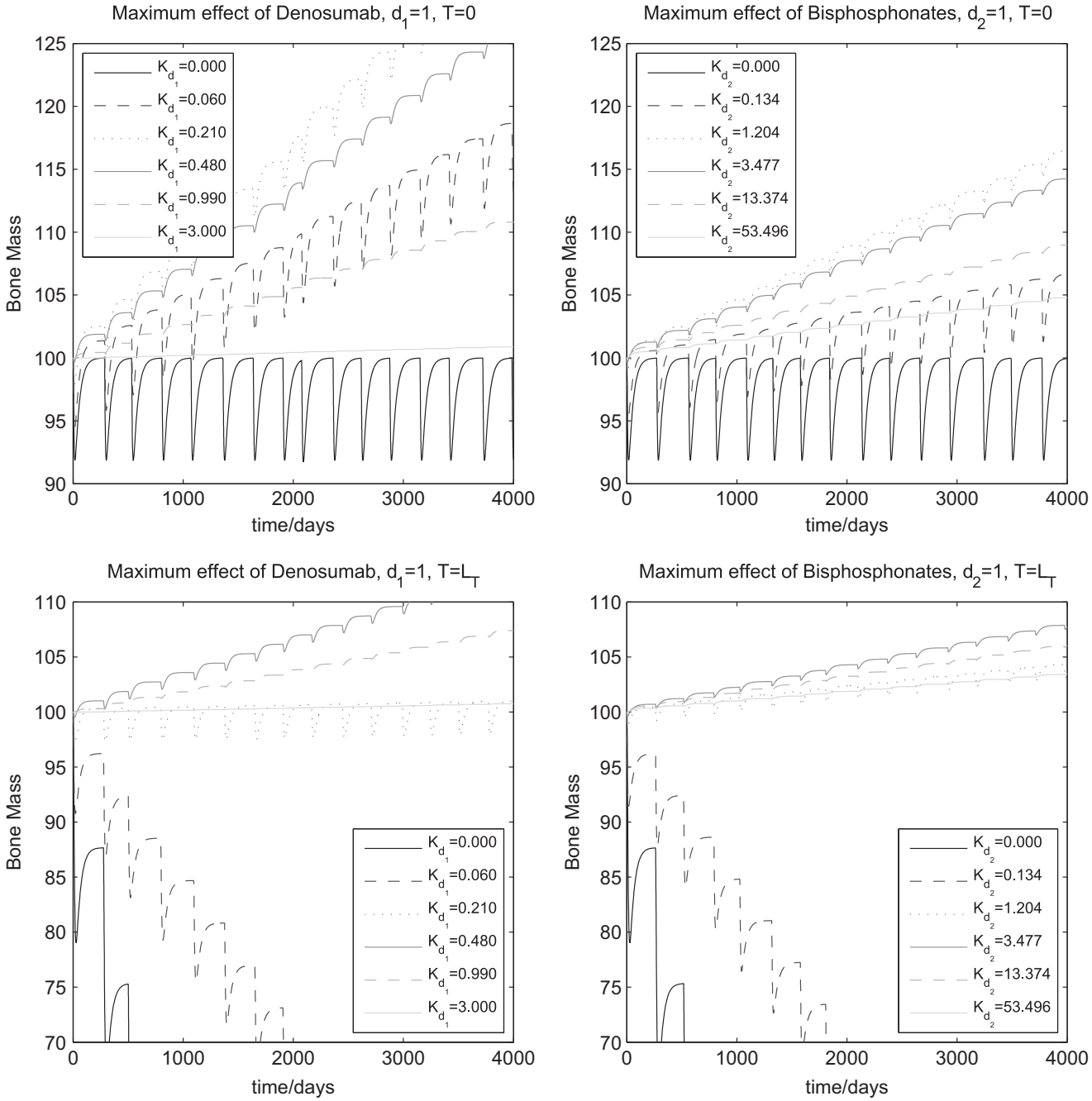

Fig. 5. Study of different maximum effect of anti-resorptive treatment with denosumab (K_{d_1}) and bisphosphonates (K_{d_2}) in bone mass dynamics for the extreme cases of no tumor ($T=0$) and maximum-sized tumor ($T=L_T$).

The bone remodeling system in the presence of tumor was simulated for anti-cancer therapy (paclitaxel) alone, then together with either denosumab or bisphosphonates, and the results are presented in Fig. 7. In all cases, the treatment starts at time t_{start} = 1200 days and is interrupted at t_{stop} = 2200 days. The values for K_{d_1} and K_{d_2} are chosen through simulation such that there is an increase in bone mass regardless of the disease burden. The parameters used for the simulation are presented in Tables 2 and 3.

Treatment with chemotherapy, represented by the full line, is able to reduce the tumor size to nearly zero and restore the normal remodeling cycle. However, because no anti-resorptive therapy is applied, as long as there are cancer cells, the bone mass will decrease due to increased bone resorption and is not recovered. Furthermore, bone resorption will induce the growth of tumor during the disrupted remodeling cycle. In case bone metastases are completely eliminated, which is not usually the case, the regular mechanisms of bone physiology would regenerate bone and increase bone mass, which is not taken into account in this model.

Anti-resorptive treatment by itself is not used for the purpose of killing cancer cells, but can at least inhibit their growth and even partially restore bone mass. Comparing the results of anti-cancer therapy together with denosumab and with bisphosphonates, represented in Fig. 7 by the dashed and dotted lines, respectively, it can be observed that, in both cases, the tumor size is greatly reduced due to the effect of anti-cancer therapy and that bone mass increases through the anti-resorptive treatment. In this setting, bone formation will be greater than bone resorption, which will result in an increase in bone mass.

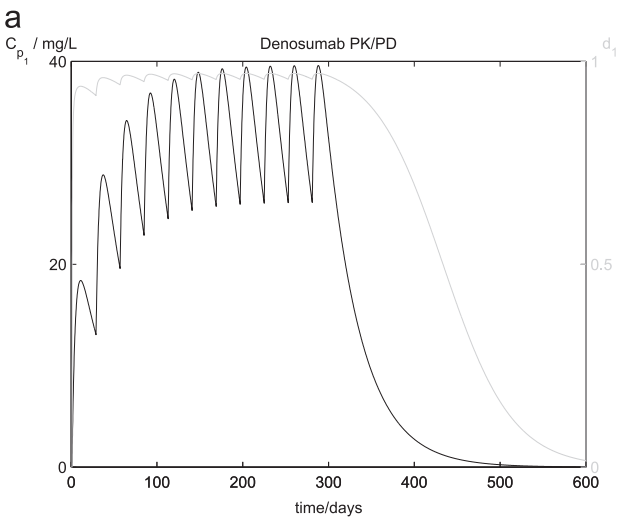

PK (C_{p_1}) and PD(d_1) for denosumab.

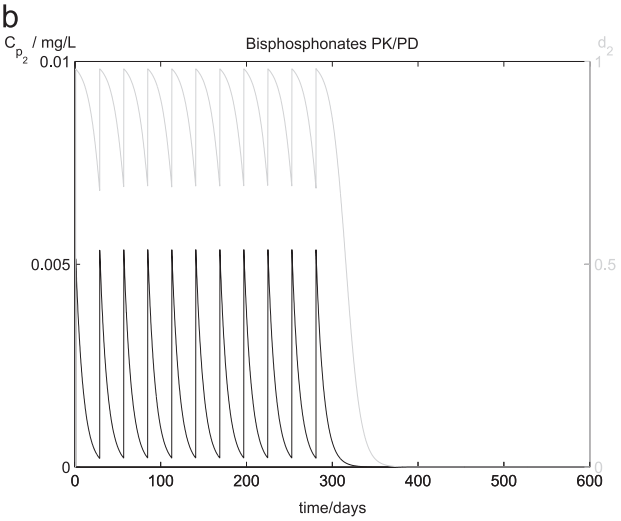

PK (C_{p_2}) and PD (d_2) for bisphosphonates.

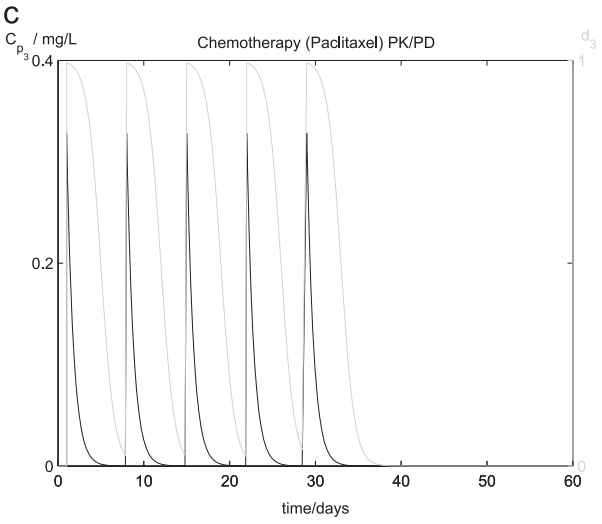

PK(C_{p_3}) and PD (d_3) for paclitaxel.

Fig. 6. PK/PD for anti-resorptive and anti-cancer therapy.

The main difference between the treatment with denosumab and bisphosphonates in this model is that the former induces a greater reduction in the number of osteoclasts than the latter, while achieving a similar number of active osteoblasts. As such, the increase in bone formation with respect to bone resorption will be greater in the treatment with denosumab than with bisphosphonates.

In any case, the tumor is usually never completely eliminated, which can lead to cases of tumor regrowth, as shown by the increase in tumor size after the treatment is stopped.

5. Conclusion

This paper proposes a model for bone remodeling in presence of bone metastases that includes novel features such as the effect of PTH in the bone remodeling dynamics and its role in activating remodeling cycles, the induction of a vicious cycle through the production of PTHrP by bone metastatic cells and the consequential increase in bone resorption, and the PK/PD of the therapies currently applied including the two main categories of anticancer and antiresorptive treatment.

The system presented here expands previously proposed models that already coupled the dynamics of the bone cells and extends them to include a mechanism that activates bone remodeling through the increase in concentration of PTH at the remodeling site, rather than simply introducing a perturbation on the initial conditions.

In order to account for the effect of the tumour on the bone dynamics, previous efforts based on altering the parameters of the system that represent the autocrine regulations are expanded, although preserving the type of stability of the resulting steady-state. By including the PTH_{pool} variable, which represents both PTH and PTHrP concentrations, it is possible to recreate the vicious cycle of bone metastases, where bone resorption promotes the

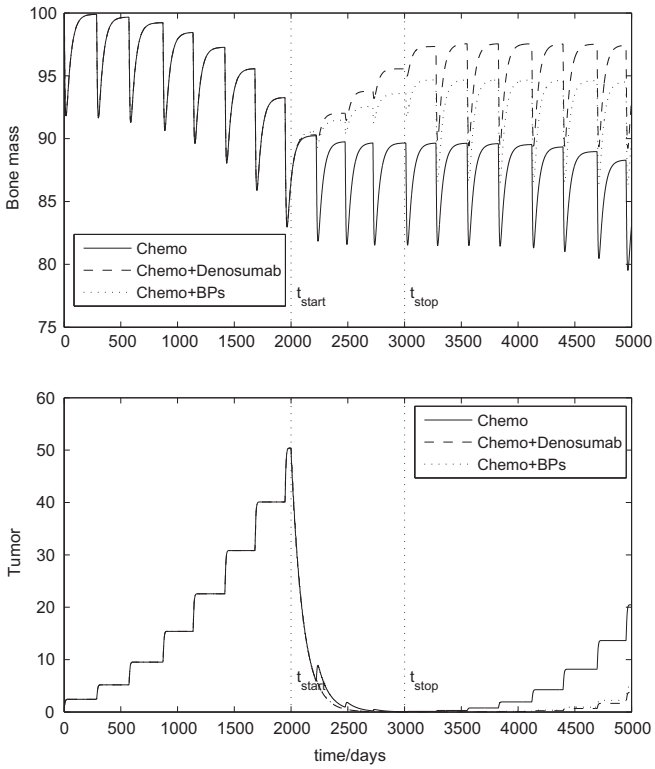

Fig. 7. Comparison of bone mass and tumor evolution in response to different kinds of treatment: anti-cancer therapy (full-line); anti-cancer therapy and denosumab (dashed-line); anti-cancer therapy and bisphosphonates (dotted-line).

growth of the tumour, which in turn increases bone resorption through PTHrP.

Moreover, the new model includes not only anticancer treatment, but also antiresorptive treatment, which can inhibit bone resorption and consequently the growth of bone metastases, an important characteristic of the bone metastatic disease and therapy not considered previously.

There are several physiological features than can be further included in the models. For example, the effect of other hormones such as oestrogen which are secreted by breast cancer cells has a known impact on the dynamics of bone remodeling. The inclusion of hormonotherapy would also contribute to a wider understanding of the coupling with these relevant proteins. Moreover, it is of the utmost importance to incorporate drug resistance in the model, in order to understand the dosages and intervals of administration that maximize the effect of the therapy, while reducing the toxicity added to the system. At a certain point, bone metastases develop mechanisms that make them independent of the bone microenvironment to grow and proliferate, which is not taken into account in the proposed model. Furthermore, it is very difficult to attribute the effects specifically to PTH or PTHrP, which are here collapsed into one variable, but the separate contribution of each could be further explored in the future. Another challenge would be to extend the model by taking into account the spatial evolution, which is of paramount importance in the understanding of bone remodeling and metastasis system.

It is expected that the computational modeling of this relevant physiological process can contribute to support clinical decisions and the design of therapeutic regimes for bone metastatic patients.

Acknowledgments

This work was supported by FCT, through IDMEC, under LAETA projects UID/EMS/50022/2013, BoneSys, CancerSys (EXPL/EMS-SIS/1954/2013), PERSEIDS (PTDC/EMS-SIS/0642/2014) , INESC-ID UID/CEC/5002/2013 and COMPETE. SV acknowledges support by Program Investigador FCT (IF/00653/2012) from FCT, co-funded by the European Social Fund (ESF) through the Operational Program Human Potential (POPH).

References

Araujo, A., Cook, L.M., Lynch, C.C., Basanta, D., 2014. An integrated computational model of the bone microenvironment in bone-metastatic prostate cancer. Cancer Res. 74, 2391–2401. http://dx.doi.org/10.1158/0008-5472.CAN-13-2652, URL ⟨http://cancerres.aacrjournals.org/content/74/9/2391.abstract⟩.

Ayati, B.P., Edwards, C.M., Webb, G.F., Wikswo, J.P., 2010. A mathematical model of bone remodeling dynamics for normal bone cell populations and myeloma bone disease. Biol. Direct 5, 28. http://dx.doi.org/10.1186/1745-6150-5-28, URL ⟨http://www.pubmedcentral.nih.gov/articlerender.fcgi?artid=2867965&tool=pmcentrez&rendertype=abstract⟩.

Boyce, B.F., 2012. Bone biology and pathology. In: Coleman, R., Abrahamsson, P.-A., Hadji, P. (Eds.), Handbook of Cancer-Related Bone Disease, 2nd ed. BioScientifica, Bristol, pp. 3–21 (Chapter 1).

Buenzli, P.R., Pivonka, P., Smith, D.W., 2011. Spatio-temporal structure of cell distribution in cortical bone multicellular units: a mathematical model. Bone 48, 918–926. http://dx.doi.org/10.1016/j.bone.2010.12.009, URL ⟨http://www.ncbi.nlm.nih.gov/pubmed/21172465⟩.

Casimiro, S., Guise, T.A., Chirgwin, J., 2009. The critical role of the bone microenvironment in cancer metastases. Mol. Cell. Endocrinol. 310, 71–81. http://dx.doi.org/10.1016/j.mce.2009.07.004, URL ⟨http://www.sciencedirect.com/science/article/pii/S0303720709003621⟩.

Chen, T., Berenson, J., Vescio, R., Swift, R., Gilchick, A., Goodin, S., LoRusso, P., Ma, P., Ravera, C., Deckert, F., Schran, H., Seaman, J., Skerjanec, A., 2002. Pharmacokinetics and pharmacodynamics of zoledronic acid in cancer patients with bone metastases. J. Clin. Pharmacol. 42, 1228–1236, URL ⟨http://www.ncbi.nlm.nih.gov/pubmed/12412821⟩.

Crockett, J.C., Rogers, M.J., Coxon, F.P., Hocking, L.J., Helfrich, M.H., 2011. Bone remodelling at a glance. J. Cell Sci. 124, 991–998. http://dx.doi.org/10.1242/jcs.063032, URL ⟨http://jcs.biologists.org/content/124/7/991⟩.

Dhillon, S., Kostrzewski, A., 2006. Basic pharmacokinetics. In: Clinical Pharmacokinetics. Pharmaceutical Press London, UK (Chapter 1), URL ⟨https://books.google.com/books?id=EUtrudCbQMwC&pgis=1⟩.

Gibiansky, L., Sutjandra, L., Doshi, S., Zheng, J., Sohn, W., Peterson, M.C., Jang, G.R., Chow, A.T., Pérez-Ruixo, J.J., 2012. Population pharmacokinetic analysis of denosumab in patients with bone metastases from solid tumours. Clin. Pharmacokinet. 51, 247–260. http://dx.doi.org/10.2165/11598090-000000000-00000, URL ⟨http://www.ncbi.nlm.nih.gov/pubmed/22420579⟩.

Haden, S.T., Brown, E.M., Hurwitz, S., Scott, J., El-Hajj Fuleihan, G., 2000. The effects of age and gender on parathyroid hormone dynamics. Clin. Endocrinol. 52, 329–338, URL ⟨http://www.ncbi.nlm.nih.gov/pubmed/10718831⟩.

Hofbauer, L.C., Rachner, T.D., Coleman, R.E., Jakob, F., 2014. Endocrine aspects of bone metastases. Lancet Diabetes Endocrinol. 2, 500–512. http://dx.doi.org/10.1016/S2213-8587(13)70203-1, URL ⟨http://linkinghub.elsevier.com/retrieve/pii/S2213858713702031⟩.

Komarova, S.V., 2005. Mathematical model of paracrine interactions between osteoclasts and osteoblasts predicts anabolic action of parathyroid hormone on bone. Endocrinology 146, 3589–3595. http://dx.doi.org/10.1210/en.2004-1642, URL ⟨http://www.ncbi.nlm.nih.gov/pubmed/15860557⟩.

Komarova, S.V., Smith, R.J., Dixon, S., Sims, S.M., Wahl, L.M., 2003. Mathematical model predicts a critical role for osteoclast autocrine regulation in the control of bone remodeling. Bone 33, 206–215. http://dx.doi.org/10.1016/S8756-3282(03)00157-1, URL ⟨http://linkinghub.elsevier.com/retrieve/pii/S8756328203001571⟩.

Lemaire, V., Tobin, F.L., Grelle, L.D., Cho, C.R., Suva, L.J., 2004. Modeling the interactions between osteoblast and osteoclast activities in bone remodeling. J. Theor. Biol. 229, 293–309. http://dx.doi.org/10.1016/j.jtbi.2004.03.023, URL ⟨http://www.ncbi.nlm.nih.gov/pubmed/15234198⟩.

Makatsoris, T., Kalofonos, H.P., 2009. The role of chemotherapy in the treatment of bone metastases. In: Kardamakis, D., Vassiliou, V., Chow, E. (Eds.), Bone Metastases. Cancer Metastasis Biology and Treatment, vol. 12. Springer Netherlands, Dordrecht, pp. 287–297, URL ⟨doi:10.1007/978-1-4020-9819-2_14⟩.

Moulopoulos, L.A., Koutoulidis, V., 2014. Bone Marrow MRI: a Pattern-Based Approach, vol. 17. Springer, Milan, Italy, URL ⟨https://books.google.com/books?id=I5FxBQAAQBAJ&pgis=1⟩.

Mundy, G.R., Edward, J.R., 2008. PTH-related peptide (PTHrP) in hypercalcemia. J. Am. Soc. Nephrol.: JASN 19, 672–675. http://dx.doi.org/10.1681/ASN.2007090981, URL ⟨http://jasn.asnjournals.org/content/19/4/672.long⟩.

Perez, E.A., Vogel, C.L., Irwin, D.H., Kirshner, J.J., Patel, R., 2001. Multicenter phase II trial of weekly paclitaxel in women with metastatic breast cancer. J. Clin.

Oncol.: Off. J. Am. Soc. Clin. Oncol. 19, 4216–4223, URL ⟨http://www.ncbi.nlm.nih.gov/pubmed/11709565⟩.

Pivonka, P., Zimak, J., Smith, D.W., Gardiner, B.S., Dunstan, C.R., Sims, N.A, Martin, T. J., Mundy, G.R., 2008. Model structure and control of bone remodeling: a theoretical study. Bone 43, 249–263. http://dx.doi.org/10.1016/j.bone.2008.03.025, URL ⟨http://www.ncbi.nlm.nih.gov/pubmed/18514606⟩.

Pivonka, P., Zimak, J., Smith, D.W., Gardiner, B.S., Dunstan, C.R., Sims, N.a., Martin, T. J., Mundy, J.R., 2010. Theoretical investigation of the role of the RANK-RANKL-OPG system in bone remodeling. J. Theor. Biol. 262, 306–316. http://dx.doi.org/10.1016/j.jtbi.2009.09.021, URL ⟨http://www.ncbi.nlm.nih.gov/pubmed/19782692⟩.

Raggatt, L.J., Partridge, N.C., 2010. Cellular and molecular mechanisms of bone remodeling. J. Biol. Chem. 285, 25103–25108. http://dx.doi.org/10.1074/jbc.R109.041087, URL ⟨http://www.pubmedcentral.nih.gov/articlerender.fcgi?artid=2919071&tool=pmcentrez&rendertype=abstract⟩.

Ryser, M.D., Komarova, S.V., Nigam, N., 2010. The cellular dynamics of bone remodeling: a mathematical model. SIAM J. Appl. Math. 70, 1899–1921. http://dx.doi.org/10.1137/090746094, URL ⟨http://epubs.siam.org/doi/abs/10.1137/090746094⟩.

Ryser, M.D., Nigam, N., Komarova, S.V., 2009. Mathematical modeling of spatio-temporal dynamics of a single bone multicellular unit. J. Bone Miner. Res.: off. J. Am. Soc. Bone Miner. Res. 24, 860–870. http://dx.doi.org/10.1359/jbmr.081229, URL ⟨http://www.ncbi.nlm.nih.gov/pubmed/19063683⟩.

Ryser, M.D., Qu, Y., Komarova, S.V, 2012. Osteoprotegerin in bone metastases: mathematical solution to the puzzle. PLoS Comput. Biol. 8, e1002703. http://dx.doi.org/10.1371/journal.pcbi.1002703, URL ⟨http://www.pubmedcentral.nih.gov/articlerender.fcgi?artid=3475686&tool=pmcentrez&rendertype=abstract⟩.

Savageau, M.A., 1988. Introduction to S-systems and the underlying power-law formalism. Math. Comput. Model. 11, 546–551. http://dx.doi.org/10.1016/0895-7177(88)90553-5, URL ⟨http://www.sciencedirect.com/science/article/pii/0895717788905535⟩.

Scheiner, S., Pivonka, P., Smith, D.W., Dunstan, C.R., Hellmich, C., 2014. Mathematical modeling of postmenopausal osteoporosis and its treatment by the anti-catabolic drug denosumab. Int. J. Numer. Methods Biomed. Eng. 30, 1–27. http://dx.doi.org/10.1002/cnm.2584, URL ⟨http://www.pubmedcentral.nih.gov/articlerender.fcgi?artid=4291103&tool=pmcentrez&rendertype=abstract⟩.

Schneider, A., Kalikin, L.M., Mattos, A.C., Keller, E.T., Allen, M.J., Pienta, K.J., McCauley, L.K., 2005. Bone turnover mediates preferential localization of prostate cancer in the skeleton. Endocrinology 146, 1727–1736. http://dx.doi.org/10.1210/en.2004-1211, URL ⟨http://www.ncbi.nlm.nih.gov/pubmed/15637291⟩.

Silva, B.C., Bilezikian, J.P., 2015. Parathyroid hormone: anabolic and catabolic actions on the skeleton. Curr. Opin. Pharmacol. 22, 41–50. http://dx.doi.org/10.1016/j.coph.2015.03.005, URL ⟨http://www.ncbi.nlm.nih.gov/pubmed/25854704⟩.

Suva, L.J., Washam, C., Nicholas, R.W., Griffin, R.J., 2011. Bone metastasis: mechanisms and therapeutic opportunities. Nat. Rev. Endocrinol. 7, 208–218. http://dx.doi.org/10.1038/nrendo.2010.227, URL ⟨http://www.pubmedcentral.nih.gov/articlerender.fcgi?artid=3134309&tool=pmcentrez&rendertype=abstract⟩.

Voorzanger-Rousselot, N., Goehrig, D., Journe, F., Doriath, V., Body, J.J., Clézardin, P., Garnero, P., 2007. Increased Dickkopf-1 expression in breast cancer bone metastases. Br. J. Cancer 97, 964–970. http://dx.doi.org/10.1038/sj.bjc.6603959, URL ⟨http://www.pubmedcentral.nih.gov/articlerender.fcgi?artid=2360424&tool=pmcentrez&rendertype=abstract⟩.

Wang, Y., Pivonka, P., Buenzli, P.R., Smith, D.W., Dunstan, C.R., 2011. Computational modeling of interactions between multiple myeloma and the bone microenvironment. PLoS One 6, e27494. http://dx.doi.org/10.1371/journal.pone.0027494, URL ⟨http://www.pubmedcentral.nih.gov/articlerender.fcgi?artid=3210790&tool=pmcentrez&rendertype=abstract⟩.

Zumsande, M., Stiefs, D., Siegmund, S., Gross, T., 2011. General analysis of mathematical models for bone remodeling. Bone 48, 907–910. http://dx.doi.org/10.1016/j.bone.2010.12.010, URL ⟨http://www.ncbi.nlm.nih.gov/pubmed/21185412⟩.